Histological changes in chronic autoimmune SKG-arthritis evaluated by quantitative three-dimensional stereological estimators

K.K. Keller[1], K. Stengaard-Pedersen[1], F. Dagnæs-Hansen[2], J.R. Nyengaard[3], S. Sakaguchi[4], E.-M. Hauge[1]

[1]Department of Rheumatology, Aarhus University Hospital, Aarhus, Denmark; [2]Institute of Medical Microbiology and Immunology, Aarhus University, Aarhus, Denmark; [3]Stereology and Electron Microscopy Laboratory, Centre for Stochastic Geometry and Advanced Bioimaging, Aarhus University Hospital, Aarhus, Denmark; [4]Department of Experimental Pathology, Institute for Frontier Medical Science, Kyoto University, Japan.

Abstract

Objective

To investigate the quantitative arthritic and bone erosive changes, including the number of osteoclasts and osteoclast precursors in the new SKG-model of inflammatory polyarthritis using three-dimensional (3D) stereological methods.

Methods

Arthritis was induced in female SKG-mice with Zymosan A. Quantitative histology was made in four control mice and four mice with arthritis euthanised after 6 and 12 weeks. The right hind paw was embedded undecalcified in methylmethacrylate and cut exhaustively generating vertical uniform random sections. A computer controlled microscope and stereological software was used for histological quantification. Total volumes were estimated according to the Cavalieri principle, total surfaces were estimated using the vertical sections design, and the number of osteoclasts was counted in a physical fractionator.

Results

The arthritis score increased during the 12-week period and was paralleled by an increase in the volume of inflammatory tissue ($r=0.96$, $p<0.001$). The number of osteoclasts on bone ($r=0.77$, $p<0.05$) and osteoclast-covered bone surface ($r=0.62$, $p<0.05$) increased resulting in a decrease in the volume of bone ($r=-0.65$, $p<0.05$). However, the number of osteoclast precursors declined between week 6 and 12 ($p<0.05$). Furthermore, the total cartilage surface ($r=-0.74$, $p<0.05$) and cartilage volume ($r=-0.74$, $p<0.05$) decreased during the 12 weeks of arthritis.

Conclusions

In this study we demonstrated changes in 3D stereological parameters of inflammatory tissue, bone erosion, osteoclasts, and cartilage in mouse paws during the course of arthritis in the SKG mouse. This is the first time 3D quantitative histology has been applied in a mouse model of rheumatoid arthritis.

Key words

osteoclasts, bone, cartilage, histology, experimental arthritis

Kresten Krarup Keller, MD
Kristian Stengaard-Pedersen, MD, DMSc
Frederik Dagnæs-Hansen, PhD
Jens Randel Nyengaard, MD, DMSc
Shimon Sakaguchi, MD, PhD
Ellen-Margrethe Hauge, MD, PhD

This work was supported by the Hørslev foundation, Clinical institute Aarhus University, the Danish Rheumatism Association, Peter Ryholts grant, the Hede Nielsens family Foundation, The Foundation for Promoting Medical Science and the Aase and Ejnar Danielsens Foundation. The Centre for Stochastic Geometry and Advanced Bioimaging is supported by the Villum Foundation.

Please address correspondence and reprint requests to:
Dr Kresten Keller,
Department of Rheumatology,
Aarhus University Hospital,
Norrebrogade 44,
DK-8000 Aarhus, Denmark.
E-mail: kresten@hotmail.com

Reprints will not be available from the author.

Received on October 27, 2010; accepted in revised form on February 11, 2011.

Competing interests: none declared.

Introduction

Rheumatoid arthritis (RA) is a chronic autoimmune disease mainly affecting the joints. One of the major reasons for joint disability is the degradation of bone. The discovery of the receptor activator of NFκB ligand (RANKL) system (1, 2) initiated research, which has elucidated the biochemical and cellular processes involved in the development of bone erosions. At the cartilage-pannus junction bone is eroded by osteoclasts under the influence of RANKL and macrophage colony-stimulating factor (M-CSF) (3). Osteoclast precursors are located in the pannus while on the bone surface only cells showing the full repertoire of osteoclast phenotype are found (4-6).

The SKG mice were first described in 2003 by Sakaguchi and co-workers (7). Due to a point mutation in the T-cells, these mice spontaneously develop arthritis unless they are kept under specific pathogen free (SPF) conditions. Arthritis can also be reproducibly initiated (8). This chronic arthritis model resembles RA in many ways including peripheral destructive polyarthritis, extraarticular manifestations, autoantibodies and elevated IL-1, IL-6 and TNF-α (7-9). Furthermore, the histology shows synovitis, pannus formation and erosions of cartilage and bone (7). The exact time for the onset of erosions is not known.

Much is known about the pathogenesis of RA from qualitative and two-dimensional (2D) histological studies on animals. These methods includes semiquantitative scoring systems, estimation of volume fractions and measurement of osteoclasts by counting Tartrate-resistant acidic phosphatase (TRAP)-positive cell profiles.

New three-dimensional (3D) stereology methods have proven useful in many research areas (10-12). These advances include a method for measuring absolute volume using the Cavalieri principle (13) and a method for counting the absolute number of cells in a tissue (the disector/fractionator) (14). So far, these methods have not been used to quantify and characterise the joint tissue changes during the course of an experimental murine model of RA.

The aim of this study was to investigate the quantitative arthritic and bone erosive changes including the number of osteoclasts and osteoclast precursors in the new SKG-model of inflammatory polyarthritis using 3D stereological methods.

Materials and methods

Animals and arthritis induction

Female SKG-mice were housed in a scantainer® (Scanbur, Denmark) in a controlled environment (21–25°C, 55+5% relative humidity, 12 h light/dark cycle) at the Animal Facility, The Faculty of Health Sciences, University of Aarhus. The animals were kept in autoclaved Makrolon® filtercages (Techniplast, Italy), with autoclaved water, and food (Altromin 1314, Germany). Diet and water were provided *ad libitum*. Autoclaved wooden chips (FinnTapvei, Finland) were used as bedding in the cages. Routine microbiological monitoring according to FELASA recommendations was performed regularly (15) securing a high health status corresponding to SPF bred animals.

Twelve 7-week-old SKG-mice were injected intraperitoneally with 2 mg Zymozan A (Sigma-Aldrich, USA) suspended in 0.5 ml saline as previously described (8). The mice were randomised to 6 or 12 weeks of arthritis. Four 13-week-old SKG-mice without arthritis served as controls for the histological evaluation.

Joint swelling was scored as previously described (7). At the end of the study all animals were anesthetised with isoflurane (Baxter, USA) and euthanised by cervical dislocation.

The study was approved by the Danish Animal Experiments Inspectorate.

Sampling and histological preparation of tissue

We wanted to investigate the course of arthritis, and therefore we made stereological sampling on mice with objective signs of arthritis. Two mice from the 6 and 12 week groups were excluded because of premature death or lack of clinical arthritis.

The right hind paw was cut 0.5 cm above the ankle joint and immersed in 70% alcohol for fixation followed by dehydration and undecalcified em-

bedding in methyl methacrylate (16). During the procedures the paws were kept cold.

Cutting was performed using the principle of vertical sectioning (17). The blocks were rotated randomly around the vertical axis and 7 µm tissue slides were cut exhaustively parallel to the vertical axis (18) on a heavy duty microtome equipped with a tungsten carbide knife. For each paw 10 levels with 12 tissue slides were obtained using the principle of systematic uniform random sampling (19). The Masson-Goldner trichrome and the enzymatic TRAP stains were used.

Microscopical evaluation

The microscope (Nikon ECLIPSE 80i, Japan) was equipped with a motorised Proscan 11™ stage (Prior, USA), a MT1201 microcator (Heidenhain, Germany), a DP72 camcorder (OLYMPUS, Denmark) and connected to a computer with the newCAST software vers. 3.4.1.0 (Visiopharm, Denmark).

Total volumes of bone, entire paw tissue and inflammatory tissue were estimated at a total magnification of ×229 on Masson-Goldner trichrome stained tissue slides (Fig. 1a). The total surface and volume of the cartilage were measured at a total magnification of ×457 on Masson-Goldner Trichrome stained tissue slides (Fig. 1b). When necessary, two different point and line grid dimensions were used for each tissue of interest to optimise sampling efficiency. The aim was to achieve between 100 and 200 points or intersections pr. paw. A total magnification of ×457 was used for counting the number of active osteoclasts (TRAP-positive cells on bone) and osteoclast precursors (TRAP-positive cells in inflammatory tissue) as well as the osteoclast-covered bone surface (Fig. 1c-d). In each paw, approximately 100 cells and 100-200 points or intersections were counted. All sampling was done by a blinded observer.

The reference regions were the entire paw distal to the tibia (bone and cartilage parameters), the entire tarsus (osteoclast and osteoclast precursors) or the entire paw including the tibia (inflammatory and total volume).

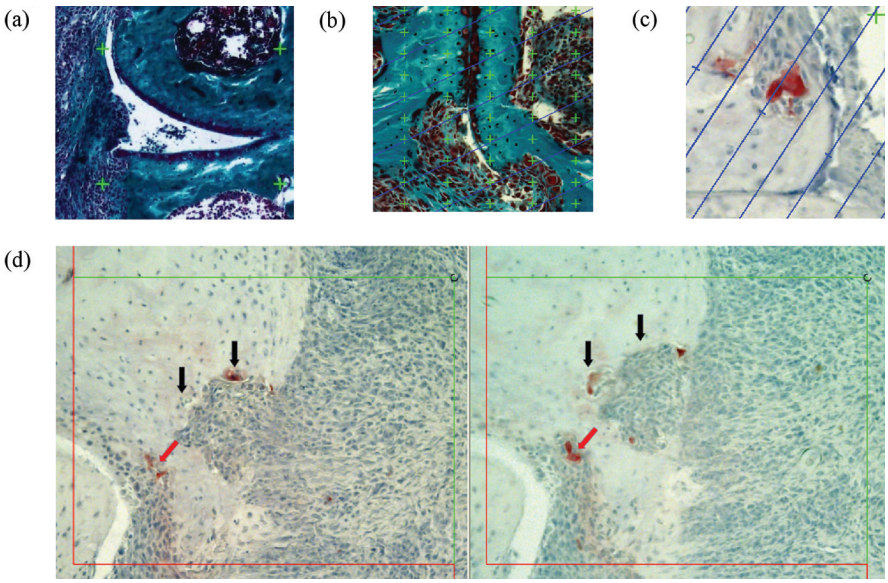

Fig. 1. Examples of different stereological count tools. Volumes are estimated by point counting (**a** and **b**). Surfaces are estimated by line counting (**b** and **c**). Number of osteoclasts is counted in a physical fractionators using two counting frames 7 µm apart (**d**). The cells seen in the reference section but not in the look-up section were counted (black arrows). Bridges, defined as cells that appears as one cell profile in the reference section and as two cell profiles in the look-up section, were counted as well (red arrow).

Volume

The absolute volume of the different compartments was measured applying the principle of Cavalieri (13):

$$V\text{archimedes} = T \cdot a(p) \cdot \sum P$$

where T is the distance between sections, a(p) is the area per point and ∑P is the total number of points counted. A(p) were 52879 µm^2 and 118978 µm^2 for bone volume, 1096 µm^2 and 2192 µm^2 for cartilage volume and 118978 µm^2 for inflammatory tissue. In this study volume was not corrected for shrinkage because tissue deformation is relatively low in plastic-embedded sections (20).

Osteoclasts and osteoclast precursors

The number of osteoclasts and osteoclast precursors were counted using the physical fractionator (21). Two neighbouring tissue slides were lined up and a 2D counting frame was used. The cells seen in the reference section but not in the look-up section were counted. A known fraction of the cells were sampled. The number of osteoclasts and osteoclast precursors as well as the number of bridges was counted in accordance with estimation of connectivety (22). A bridge is defined as a cell that appears as one cell profile in the reference section and as two cell profiles in the look-up section.

The total number of osteoclasts was estimated by:

$$N(osteoclasts) = \frac{\sum Is - \sum Br}{2} \cdot \frac{1}{ssf} \cdot \frac{1}{asf}$$

where Is (island) is the number of cells counted and Br (bridge) is where one cell profile turns into two cell profiles. ∑Is - ∑Br is divided by 2 because each pair of sections is counted both ways. Ssf is the section sampling fraction and asf is the area sampling fraction.

Surface

Surfaces were estimated according to the principles of the vertical sections design (17):

$$S = 2 \times t \cdot \frac{a}{l} \cdot \sum I$$

where t is the section thickness, a/l is the area pr length and ∑I is the number of intercepts between the surface and the line grid. a/l is 29.9 µm and 59.7 µm for cartilage surface and 29.9 µm for osteoclast-covered bone surface.

Coefficient of error

The precision of the estimates of volume are given by the coefficient of error

(CE), which is a function of two independent factors (23):

$$Var_{Noise} = 0.0724 \cdot \left(b/\sqrt{a}\right) \cdot \sqrt{n \cdot \sum p}$$

where b/√a is a shape factor, n is the number of tissue slides and ∑P is the number of points counted in the entire paw. Shape factors for the different tissues were obtained by comparing the shape of the profiles with a nomogram (19). The Variance of Noise (Var_{Noise}) is the variance of point counting.
The other factor is:

$$Var_{(\sum a)} = \frac{3(A - Var_{Noise}) - 4B + C}{240}$$

where $A = \sum P_i \cdot P_i$, $B = \sum P_i \cdot P_{i+1}$ and $C = \sum P_i \cdot P_{i+2}$

The variance of the area ($Var_{(\sum a)}$) is the variance of how the area of the tissue vary from section to section. The CE is then given by:

$$CE\left(\sum P\right) = \frac{\sqrt{Var_{Noise} + Var_{(\sum a)}}}{\sum P}$$

CE values for estimating number of osteoclasts and osteoclast precursors were obtained by switching P_i with Is - Br in the above mentioned formulas. In addition Var_{Noise} equals Is + Br (24).
CE for surface estimation can be measured using the formula below (25).

$$CE = \sqrt{\frac{n}{n-1}\left(\frac{\sum P^2}{(\sum P)^2} + \frac{\sum I^2}{(\sum I)^2} - \frac{2\sum P \cdot I}{\sum P \cdot \sum I}\right)}$$

Where n equals the number of sections, ∑I is the number of intercepts between the surface and the line grid and ∑P is the number of points counted in the reference volume. For cartilage surface the reference volume equals cartilage volume, and for osteoclast-covered bone surface the reference volume is the tarsal bone volume.
Average CE for the parameters was estimated as follows:

$$CE = \sqrt{\frac{CE_1^2 + CE_2^2 \ldots\ldots + CE_n^2}{n}}$$

Where CE_1 was the CE of a specific paw and *n* was the number of paws in the study.
In case of rare events (*e.g.* number of osteoclasts in paws of control mice) the CE was not included in the average CE.

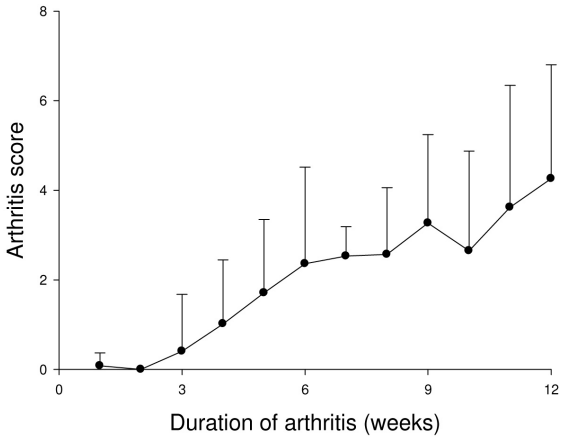

Fig. 2. Arthritis score in the arthritic SKG-mice. Arthritis was induced with intraperitoneal injection of Zymosan A in SKG-mice (n=12 mice). Data are shown as mean plus standard deviations.

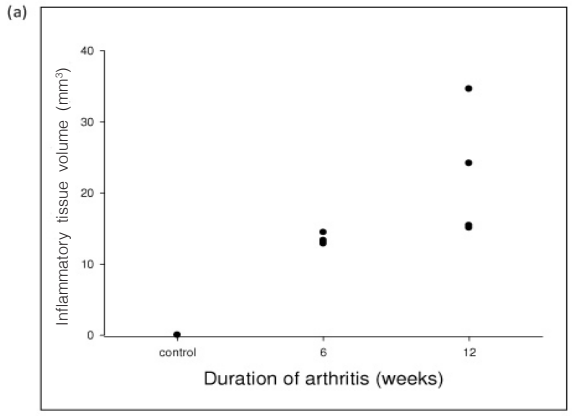

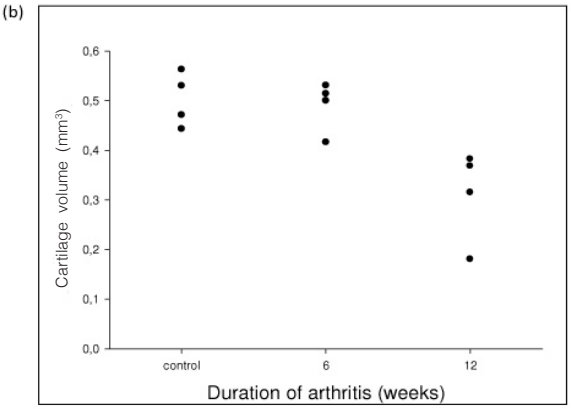

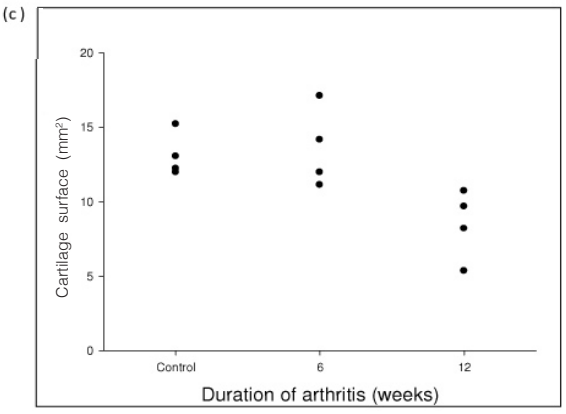

Fig. 3. Connection between duration of arthritis and inflammation and cartilage parameters. Volume of cartilage and inflammation and surface of cartilage were estimated using stereological counting tools. Data are analysed using spearman's rank correlation. The correlation coefficient *r* and the *p*-value are provided. **a**) r=0.96 and $p<0.001$, **b**) r=-0.74 and $p<0.05$, **c**) r=-0.74 and $p<0.05$

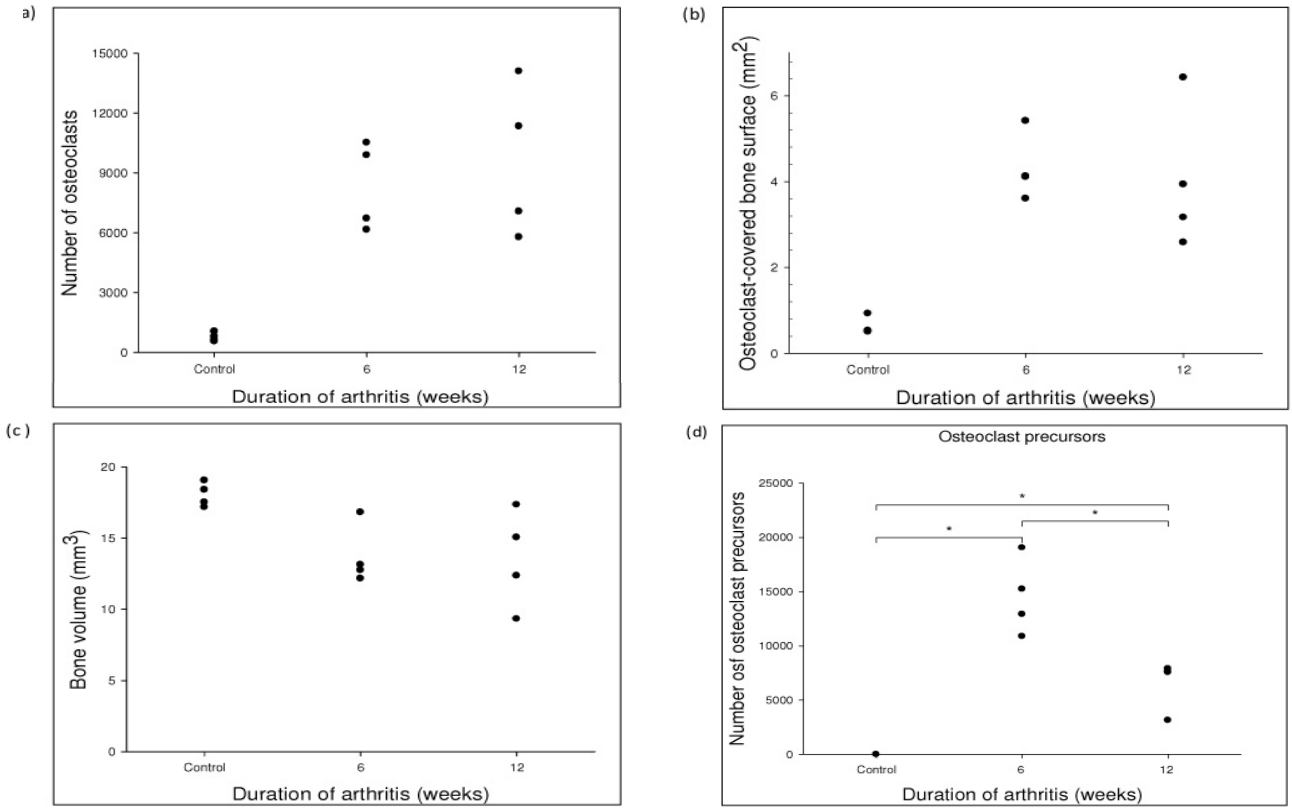

Fig. 4. Connection between duration of arthritis and bone parameters. Number of osteoclasts, osteoclast precursors, volume of bone and osteoclast-covered bone surface were estimated using stereological counting tools. Data are analysed using spearman's rank correlation (**a-c**). The correlation coefficient r and the *p*-value are provided. The number of osteoclast precursors were analysed using Kruskal-Wallis one-way analysis of variance (**d**). Because the result was significant ($p<0.001$), individual groups were compared using Mann-Whitney U-test. a) r=0.77 and $p<0.05$, b) r=0.62 and $p<0.05$, c) r=-0.65 and $p<0.05$, d) *Indicates $p<0.05$ comparing two groups.

For high CE values the proportion between the CE and the total coefficient of variance (total CV) was estimated in order to find the importance of the CE in proportion to the total CV. Values in the range $0.2<CE^2/total\ CV^2<0.5$ were acceptable.

Statistics

The software packages SIGMASTAT 3.5 and SIGMAPLOT 10.0 were used. Data were compared using Spearman's rank correlation for increasing or decreasing values. For data which did not fulfill these criteria, Kruskal-Wallis one way analysis of variance was used, and if the result was significant, groups were compared using the Mann-Whitney U-test. Data are given as the correlation coefficient (r) and median (range). *P*-values less than 0.05 were considered statistically significant.

Results

Arthritis

Arthritis developed between week one and six, and the arthritis score continued to increase throughout the study (Fig. 2). Joint swelling started primarily in the ankles and wrists, and as the disease progressed, it spread to the finger joints. In addition to arthritis, we observed unclean fur in many animals, warm and scaled tail in a few. No extraarticular manifestations were observed.

Histology

The increase in arthritis score during the 12-week period was paralleled by an increase in the volume of inflammatory tissue (r=0.96, $p<0.001$). Furthermore, the total cartilage surface (r=-0.74, $p<0.05$) and cartilage volume (r=-0.74, $p<0.05$) decreased during the 12 weeks of arthritis (Fig. 3a-c).

The number of osteoclasts on the bone surface (r=0.77, $p<0.05$) and osteoclast-covered bone surface (r=0.62, $p<0.05$) increased significantly, while a decrease in bone volume was seen (r=-0.65, $p<0.05$) (Fig. 4a-c). However, the number of osteoclast precursors did not increase with the duration of arthritis (Fig. 4d). The number of osteoclast precursors differed significantly between the groups when compared with the Kruskal-Wallis test ($p<0.001$), and the Mann-Whitney U-test showed a significant increase in osteoclast precursors from control group (0(0-0)) until week 6 (14100 (10900–19000)) ($p<0.05$), followed by a decline between week 6 (14100 (10900–19000)), and 12 (7610 (3130–7890)) ($p<0.05$). Representative pictures of the arthritic changes are shown in Figure 5.

CE

CE values are given in Table I. CE for the volume parameters were quite acceptable with values less than 5%. CE for number estimation was approximately 10%. Finally, the values for surface estimation were 12.3% (Cartilage) and 18.6% (osteoclasts). For osteoclast surface, the ratio $CE^2/total\ CV^2$ was 0.46 which we find acceptable.

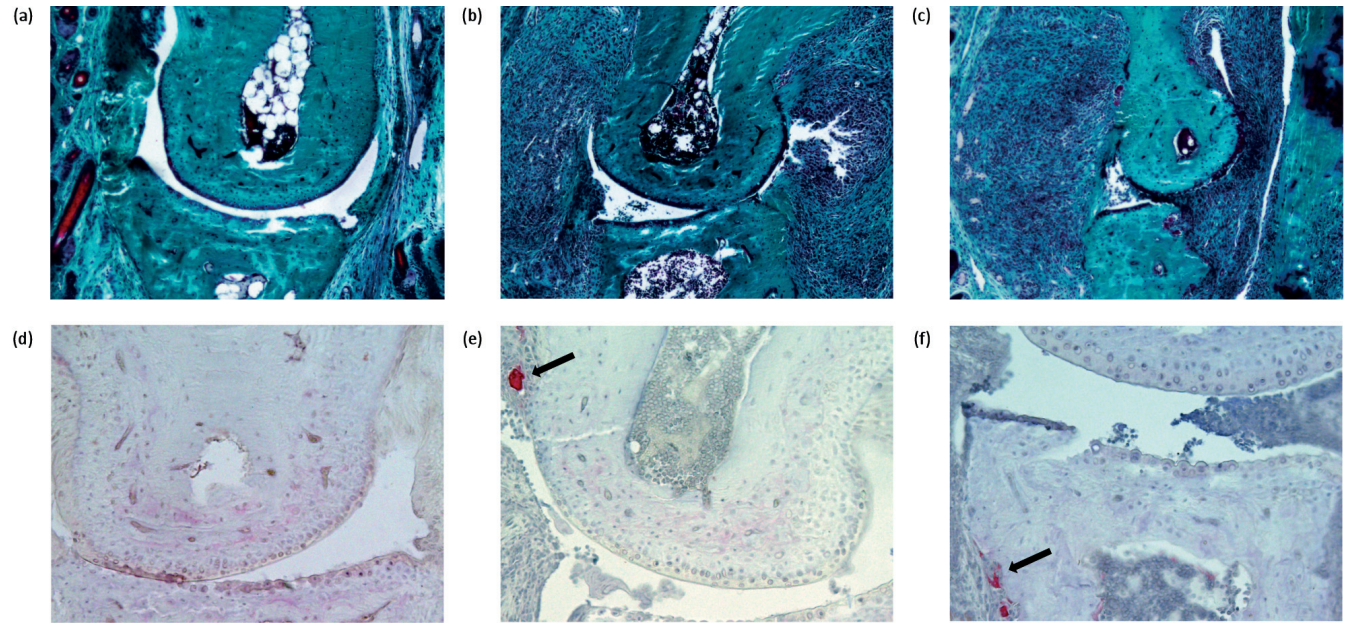

Fig. 5. Arthritic changes in the interphalangeal joints in SKG mice. Development of arthritis is demonstrated with the Masson-Goldner trichrome staining for both control (**a**), 6-week arthritis (**b**) and 12-week arthritis (**c**). The enzymatic TRAP staining was used to demonstrate osteoclasts in control animals (**d**) and after 6 weeks (**e**) and 12 weeks of arthritis (**f**). Osteoclasts are marked with black arrows.

Table I. The precision of the estimates are given by the average coefficient of error (CE) for the different parameters.

Parameter	CE
Bone volume	2.5
Number of TRAP-positive cells on bone	10.2
Number of TRAP-positive cells in inflammatory tissue	10.3
Bone surface covered by TRAP-positive cells	18.6
Volume of inflammatory tissue	3.9
Cartilage volume	4.3
Cartilage surface	12.3

CE values are given as percentages.

Discussion

In the present study we showed that the SKG-model of autoimmune polyarthritis in mice developed osteoclastic bone erosion leading to loss of bone. The loss of bone, increase in osteoclast number, and increase in osteoclast-covered bone surface continued in the chronic stage although fewer osteoclast precursors were present in the inflamed synovium.

The exact time for the onset of erosions in SKG-arthritis is not known, but it is later than in the collagen induced arthritis model where the joints are extensively eroded 3–4 weeks after onset of arthritis (26). Consequently the SKG-model seems suitable to investigate the degradation of bone and cartilage in chronic polyarthritis, as well as the importance of the osteoclast during this process. Earlier reports have stated that the SKG-mice have severe ankylosing arthritis 14 weeks after arthritis induction with Zymosan A (8). Thus, we used 12 weeks as an example of late stage disease and 6 weeks as an example of early but chronic disease. Bone loss was prominent and seems to be present 6 weeks after arthritis induction. However loss of cartilage also occurred. Cartilage degradation in RA is mainly elicited by attachment of synovial fibroblasts capable of releasing metalloproteinases at the cartilage-pannus junction (27). Judged by the histology, this also seems to be the case in the SKG-model. Our data indicates that cartilage degradation may start later than bone degradation in the SKG-mice.

Bone erosion progresses although osteoclastogenesis slows, and therefore bone erosion might be less dependent on osteoclastogenesis in the late stage of disease. In collagen-induced arthritis and adjuvant-induced arthritis, the number of osteoclast precursors peak after five and 10 days followed by a decline (28). This observation may be explained by reduced recruitment of osteoclast precursors to the joint in the late stage of arthritis, or it may simply be the evidence of a steady state in the osteoclastogenesis. It is well known how cells from the monocyte/macrophage lineage differentiate into mature osteoclasts under the influence of RANKL and M-CSF (29). However less is known about how the precursors are actually committed to enter the joint (30). The fact that both clinical arthritis score and inflammatory volume estimated by stereological estimators remained elevated indicates that the recruitment of osteoclast precursors to the joint might be partly uncoupled from the inflammatory process.

Unlike previous reports we found that arthritis did not develop in all mice. A fact that could be attributed to the 10-20% risk of misplaced intraperitoneal injections (31, 32). Because we did not make stereological assessment on these mice our results should be interpreted as an analysis of a subpopulation with objective signs of arthritis. The small number of animals in the study means that our results must be confirmed in a larger study. In our work as well as

previous studies (8), arthritis did not develop in all mice until 6 weeks after arthritis induction. A recent study demonstrated that arthritis in the SKG-mice can also be stimulated by triggering the lectin pathway of complement with mannan (33). Arthritis was seen in all animals after 2 weeks and the arthritis score became stable after 3 weeks. Hence inducing arthritis with mannan might be ideal for evaluating the effect of new therapies.

For the first time, design-based stereological principles have been implemented to a mouse model of rheumatoid arthritis. The Cavalieri principle was used to estimate the absolute volume of different compartments, thereby avoiding the so-called reference trap (34). When measuring volume fractions it is unclear whether the changes are due to changes in the tissue of interest or the total volume. This is exemplified by the fact that the total volume will increase in arthritis possibly leading to an overestimation of the changes in for example the relative volume of cartilage. Using the stereological method this problem is overcome. Three basic conditions have to be fulfilled before using the Cavalieri estimator: 1) the position of the first slice hitting the object must be random; 2) the slices are parallel; 3) the thickness of the slices is constant (19).

Estimation of the total number of osteoclasts and osteoclast precursors were done using the physical fractionator. We are the first group to report the use of this method for estimating the number of osteoclasts in arthritis research. The advantage of the fractionator compared to other methods, is that the results are not dependent on changes in the reference volume or changes in cell size/shape. For example if one counted cells in a single section the estimate would be larger if the cells were big because they would have a larger possibility of being present in a single tissue slide.

Previous studies have shown that between 100 and 200 counts and 7-10 tissue slides per animal are enough to get a low CE (19, 35, 36). In our study this proved to be true since all CE values were acceptable except for the CE of bone surface covered by TRAP-positive cells. CE for surface depends mainly on the relationship between the surface and the reference volume and less of the number of lines counted. When taking the total CV into account the CE for cartilage surface was acceptable as well. Concerning osteoclast counting a CE of approximately 10% was acceptable taken into account workload, since cell counting is very time consuming. For the same reason the tarsus was chosen for estimation of osteoclast number instead of the whole paw.

The so-called rare events in counting were not included in the average CE values because when a paw is counted and the parameter of interest is very scarce the resulting CE will always be high. Aiming at a lower CE will increase the workload substantially with only a slightly greater chance of finding a difference.

The above described new methods require special equipment and are more expensive and time consuming than traditional methods. As stated above the main advantage of the techniques is the third dimension in counting, translating the 2D information directly into true 3D information for the entire paw.

In summary, we demonstrated the changes in 3D stereological parameters in mouse paws during the course of arthritis in the SKG mouse showing presence of inflammatory tissue, increased bone erosion, increased number of osteoclasts, and loss of cartilage. This is the first time 3D quantitative histology was applied in a mouse model of RA. The methods proved valuable, and are expected to be important for future studies of the *in vivo* effect of anti-inflammatory and anti-resorptive interventions in experimental arthritis.

Acknowledgements

The authors are grateful to the technical assistance of Jette Barlach and Dorthe Clausen. We are also thankful for the technical assistance of Ernst-Martin Fuchtbauer, the Danish Centre for Transgenic Mice.

References

1. LACEY DL, TIMMS E, TAN HL *et al.*: Osteoprotegerin ligand is a cytokine that regulates osteoclast differentiation and activation. *Cell* 1998; 93: 165-76.
2. YASUDA H, SHIMA N, NAKAGAWA N *et al.*: Osteoclast differentiation factor is a ligand for osteoprotegerin/osteoclastogenesis-inhibitory factor and is identical to TRANCE/RANKL. *Proc Natl Acad Sci USA* 1998; 95: 3597-602.
3. SCHETT G: Osteoimmunology in rheumatic diseases. *Arthritis Res Ther* 2009; 11: 210.
4. GRAVALLESE EM, HARADA Y, WANG JT, GORN AH, THORNHILL TS, GOLDRING SR: Identification of cell types responsible for bone resorption in rheumatoid arthritis and juvenile rheumatoid arthritis. *Am J Pathol* 1998; 152: 943-51.
5. SUZUKI M, SUZUKI M, UETSUKA K, SHINOZUKA J, NAKAYAMA H, DOI K: Changes in location and number of tartrate-resistant acid phosphatase (TRAP)-positive cells during the development of type II collagen-induced arthritis in DBA/1J mice. *Exp Anim* 1998; 47: 211-4.
6. ROMAS E, BAKHAREVSKI O, HARDS DK *et al.*: Expression of osteoclast differentiation factor at sites of bone erosion in collagen-induced arthritis. *Arthritis Rheum* 2000; 43: 821-6.
7. SAKAGUCHI N, TAKAHASHI T, HATA H *et al.*: Altered thymic T-cell selection due to a mutation of the ZAP-70 gene causes autoimmune arthritis in mice. *Nature* 2003; 426: 454-60.
8. KOBAYASHI K, SUDA T, NAN-YA K, SAKAGUCHI N, SAKAGUCHI S, MIKI I: Cytokine production profile of splenocytes derived from zymosan A-treated SKG mice developing arthritis. *Inflamm Res* 2006; 55: 335-41.
9. HATA H, SAKAGUCHI N, YOSHITOMI H *et al.*: Distinct contribution of IL-6, TNF-alpha, IL-1, and IL-10 to T cell-mediated spontaneous autoimmune arthritis in mice. *J Clin Invest* 2004; 114: 582-8.
10. NYENGAARD JR, FLYVBJERG A, RASCH R: The impact of renal growth, regression and regrowth in experimental diabetes mellitus on number and size of proximal and distal tubular cells in the rat kidney. *Diabetologia* 1993; 36: 1126-31.
11. TANG Y, NYENGAARD JR, ANDERSEN JB, BAANDRUP U, GUNDERSEN HJ: The application of stereological methods for estimating structural parameters in the human heart. *Anat Rec (Hoboken)* 2009; 292: 1630-47.
12. HYDE DM, TYLER NK, PLOPPER CG: Morphometry of the respiratory tract: avoiding the sampling, size, orientation, and reference traps. *Toxicol Pathol* 2007; 35: 41-8.
13. GUNDERSEN HJ, BENDTSEN TF, KORBO L *et al.*: Some new, simple and efficient stereological methods and their use in pathological research and diagnosis. *APMIS* 1988; 96: 379-94.
14. STERIO DC: The unbiased estimation of number and sizes of arbitrary particles using the disector. *J Microsc* 1984; 134: 127-36.
15. REHBINDER C, BANEUX P, FORBES D *et al.*: FELASA recommendations for the health monitoring of mouse, rat, hamster, gerbil, guinea pig and rabbit experimental units. Report of the Federation of European Laboratory Animal Science Associations (FELASA) Working Group on Animal Health accepted by the FELASA Board of

Management, November 1995. *Lab Anim* 1996; 30: 193-208.
16. ERBEN RG: Trabecular and endocortical bone surfaces in the rat: modeling or remodeling? *Anat Rec* 1996; 246: 39-46.
17. BADDELEY AJ, GUNDERSEN HJ, CRUZ-ORIVE LM: Estimation of surface area from vertical sections. *J Microsc* 1986; 142: 259-76.
18. VESTERBY A, KRAGSTRUP J, GUNDERSEN HJ, MELSEN F: Unbiased stereologic estimation of surface density in bone using vertical sections. *Bone* 1987; 8: 13-7.
19. GUNDERSEN HJ, JENSEN EB: The efficiency of systematic sampling in stereology and its prediction. *J Microsc* 1987; 147: 229-63.
20. DORPH-PETERSEN KA, NYENGAARD JR, GUNDERSEN HJ: Tissue shrinkage and unbiased stereological estimation of particle number and size. *J Microsc* 2001; 204: 232-46.
21. GUNDERSEN HJ: Stereology of arbitrary particles. A review of unbiased number and size estimators and the presentation of some new ones, in memory of William R. Thompson. *J Microsc* 1986; 143: 3-45.
22. GUNDERSEN HJ, BOYCE RW, NYENGAARD JR, ODGAARD A: The Conneulor: unbiased estimation of connectivity using physical disectors under projection. *Bone* 1993; 14: 217-22.
23. GUNDERSEN HJ, JENSEN EB, KIEU K, NIELSEN J: The efficiency of systematic sampling in stereology--reconsidered. *J Microsc* 1999; 193: 199-211.
24. NYENGAARD JR: Stereologic methods and their application in kidney research. *J Am Soc Nephrol* 1999; 10: 1100-23.
25. KROUSTRUP JP, GUNDERSEN HJ: Sampling problems in an heterogeneous organ: quantitation of relative and total volume of pancreatic islets by light microscopy. *J Microsc* 1983; 132: 43-55.
26. HOLMDAHLR, BOCKERMANN R, BACKLUND J, YAMADA H: The molecular pathogenesis of collagen-induced arthritis in mice--a model for rheumatoid arthritis. *Ageing Res Rev* 2002; 1: 135-47.
27. OTERO M, GOLDRING MB: Cells of the synovium in rheumatoid arthritis. Chondrocytes. *Arthritis Res Ther* 2007; 9: 220.
28. SCHETT G, STOLINA M, BOLON B *et al*.: Analysis of the kinetics of osteoclastogenesis in arthritic rats. *Arthritis Rheum* 2005; 52: 3192-201.
29. SCHETT G: Cells of the synovium in rheumatoid arthritis. Osteoclasts. *Arthritis Res Ther* 2007; 9: 203.
30. BOYCE BF, SCHWARZ EM, XING L: Osteoclast precursors: cytokine-stimulated immunomodulators of inflammatory bone disease. *Curr Opin Rheumatol* 2006; 18: 427-32.
31. ARIOLI V, ROSSI E: Errors related to different techniques of intraperitoneal injection in mice. *Appl Microbiol* 1970; 19: 704-5.
32. GAINES DAS R, NORTH D: Implications of experimental technique for analysis and interpretation of data from animal experiments: outliers and increased variability resulting from failure of intraperitoneal injection procedures. *Lab Anim* 2007; 41: 312-20.
33. HASHIMOTO M, HIROTA K, YOSHITOMI H *et al*.: Complement drives Th17 cell differentiation and triggers autoimmune arthritis. *J Exp Med* 2010; 207: 1135-43.
34. BRAENDGAARD H, GUNDERSEN HJ: The impact of recent stereological advances on quantitative studies of the nervous system. *J Neurosci Methods* 1986; 18: 39-78.
35. PAKKENBERG B, GUNDERSEN HJ: Total number of neurons and glial cells in human brain nuclei estimated by the disector and the fractionator. *J Microsc* 1988; 150: 1-20.
36. MICHEL RP, CRUZ-ORIVE LM: Application of the Cavalieri principle and vertical sections method to lung: estimation of volume and pleural surface area. *J Microsc* 1988; 150: 117-36.